METABOLISM CLINICAL AND EXPERIMENTAL 60 (2011) 1757–1766

Available at www.sciencedirect.com

Metabolism

www.metabolismjournal.com

Basic Science

Nebivolol improves insulin sensitivity in the TGR(Ren2)27 rat

Camila Manrique[a,1], Guido Lastra[a,1], Javad Habibi[a,b,1], Lakshmi Pulakat[a], Rebecca Schneider[a,b], William Durante[c], Roger Tilmon[a], Jenna Rehmer[a], Melvin R. Hayden[a], Carlos M. Ferrario[d], Adam Whaley-Connell[a,b], James R. Sowers[a,b,c,*]

[a] Diabetes Cardiovascular Center of Excellence, University of Missouri-Columbia School of Medicine, Columbia, MO 65212, USA
[b] Research Service, Harry S. Truman Veterans Affairs Medical Center, Columbia, MO 65201, USA
[c] Medical Pharmacology and Physiology, University of Missouri-Columbia School of Medicine, Columbia, MO 65212, USA
[d] Bowman Gray School of Medicine, Wake Forest University, Winston-Salem, NC 27157, USA

ARTICLE INFO

Article history:
Received 21 January 2011
Accepted 16 April 2011

ABSTRACT

Hypertension is often associated with increased oxidative stress and systemic insulin resistance. Use of β-adrenergic receptor blockers in hypertension is limited because of potential negative influence on insulin sensitivity and glucose homeostasis. We sought to determine the impact of nebivolol, a selective vasodilatory β_1-adrenergic blocker, on whole-body insulin sensitivity, skeletal muscle oxidative stress, insulin signaling, and glucose transport in the transgenic TG(mRen2)27 rat (Ren2). This rodent model manifests increased tissue renin angiotensin expression, excess oxidative stress, and whole-body insulin resistance. Young (age, 6-9 weeks) Ren2 and age-matched Sprague-Dawley control rats were treated with nebivolol 10 mg/(kg d) or placebo for 21 days. Basal measurements were obtained for glucose and insulin to calculate the homeostasis model assessment. In addition, insulin metabolic signaling, nicotinamide adenine dinucleotide phosphate (NADPH) oxidase activity, reactive oxygen species, and ultrastructural changes as evaluated by transmission electron microscopy were examined ex vivo in skeletal muscle tissue. The Ren2 rat demonstrated systemic insulin resistance as examined by the homeostasis model

Author contributions: Camila Manrique, Javad Habibi, and Guido Lastra: These are the leading authors, who actively and equally participated in the design, planning, and conduction of the study, as well as in the data collection and analysis. These authors also actively led the writing and edition of the manuscript. Lakshmi Pulakat: This author was actively involved in the analysis and interpretation of the data, as well as in the planning of the manuscript. Rebecca Schneider: As laboratory manager, this author was the leader in the collection of data in all the animals and tissues used in this paper. William Durante: Dr Durante participated in the collection and analysis of data pertaining to oxidative stress in our tissues. Roger Tilmon: This author actively participated in the production of immunohistochemistry data. Jenna Rehmer: This author participated in the acquisition of Western blot data used to evaluate insulin signaling in our skeletal muscle samples. Melvin R. Hayden: This author was actively involved and led the collection of transmission electron microscopy data, as well as its analysis, in our samples. Carlos M. Ferrario: Dr Ferrario kindly provided the Ren2 rats used in our experiments. Adam Whaley-Connell: Dr Whaley-Connell provided daily mentorship in completion of the studies, assistance in the development of our manuscript, and financial support through CDA funds with the Department of Veteran's Affairs. James R. Sowers: Dr Sowers is the senior author and was the leader in the planning, conduction of the study, as well as in the analysis of the data and in the writing and correction of the manuscript. Our study was made possible by Dr Sowers' funding obtained through the National Institutes of Health and Forest Laboratories.

* *Corresponding author*. University of Missouri-Columbia School of Medicine, D109 HSC Diabetes Center, Columbia, MO 65212, USA. Tel.: +1 573 882 2273; fax: +1 573 884 5530.
E-mail address: sowersj@health.missouri.edu (J.R. Sowers).
[1] Authors contributed equally to this paper.

0026-0495/$ – see front matter
doi:10.1016/j.metabol.2011.04.009

assessment, along with impaired insulin metabolic signaling in skeletal muscle. This was associated with increased oxidative stress and mitochondrial remodeling. Treatment with nebivolol was associated with improvement in insulin resistance and decreased NADPH oxidase activity/levels of reactive oxygen species in skeletal muscle tissue. Nebivolol treatment for 3 weeks reduces NADPH oxidase activity and improves systemic insulin resistance in concert with reduced oxidative stress in skeletal muscle in a young rodent model of hypertension, insulin resistance, and enhanced tissue RAS expression.

1. Introduction

Hypertension frequently coexists with insulin resistance and type 2 diabetes mellitus: it is estimated that approximately 50% of hypertensive patients have evidence of insulin resistance [1,2]. In several population-based studies, elevated serum insulin levels predict higher blood pressures and future development of hypertension [1,3-5]. Insulin resistance that is associated with hypertension is characterized by impaired insulin metabolic signaling that results in reduction of glucose transport and decreased nonoxidative glucose metabolism in insulin-sensitive tissues such as skeletal muscle [2,3].

Activation of the renin-angiotensin-aldosterone system (RAAS) leads to increased generation of reactive oxygen species (ROS) in several tissues [3]. The consequent increase in oxidative stress, in turn, contributes to a decrease in insulin metabolic signaling in various insulin-responsive tissues [3]. In skeletal muscle and cardiovascular tissue, the enzymatic complex nicotinamide adenine dinucleotide phosphate (NADPH) oxidase is critical in mediating RAAS generation of ROS and impaired insulin metabolic signaling [1,3,6-10]. Reactive oxygen species also diminishes the bioavailability of nitric oxide (NO) through conversion of locally released NO to peroxynitrite ($ONOO^-$) [3]. This reduction in bioavailable NO contributes to microvascular dysfunction that results in decreased delivery of insulin and glucose to skeletal muscle tissue and other insulin-sensitive tissues, resulting in decreased insulin-mediated glucose transport [2,11-13]. The resulting decrease in insulin metabolic signaling is characterized by impaired insulin receptor substrate 1 (IRS-1) engagement with the p85 regulatory component of phosphoinositol 3-kinase (PI3K) and protein kinase B phosphorylation/activation [2]. Thus, strategies to reduce oxidative stress and increase bioavailable NO have considerable potential utility in treating hypertension in conditions characterized by insulin resistance [4,2].

Therapeutic strategies that inhibit the RAAS, as well as attenuation of oxidant stress, have been shown to improve insulin sensitivity in hypertensive rodents [6,14-16]. On the other hand, classic β-adrenergic receptor blockers have been shown to aggravate insulin resistance in hypertensive individuals [4,17]. In the context of treatment of hypertension in insulin-resistant individuals, nebivolol, a selective β_1-adrenergic blocker with vasodilatory and antioxidant properties, has been shown to improve oxidant stress and systemic insulin sensitivity, likely through reductions in NADPH oxidase activity and enhancement of endothelial NO synthase activity [18-20]. Thereby, we hypothesized that in vivo treatment with nebivolol in a rodent model of RAAS overactivation would improve systemic insulin sensitivity and insulin-stimulated glucose utilization through reductions in NADPH oxidase–dependent oxidant stress. To address this hypothesis, we used the transgenic TG(mRen2)27 (Ren2) rat model that manifests increased tissue renin and angiotensin (Ang II) expression, hypertension, and systemic insulin resistance [6,15,16].

2. Materials and methods

2.1. Animals and treatments

All animal procedures were approved by the University of Missouri animal care and use committees and housed in accordance with National Institutes of Health guidelines. Male transgenic TG(mRen2)27 (Ren2) rats (6-9 weeks of age) and age-matched Sprague-Dawley (SD) littermates were randomly assigned to placebo (Ren2-C and SD-C) or nebivolol treatment (Ren2-N and SD-N, between 5 and 13 animals per group) paradigms. Ren2-N and SD-N rats received 10 mg/kg/d of nebivolol released via an implanted osmotic minipump for 21 days. The statistical power was calculated to detect statistically significant differences in our primary outcome, which was systemic insulin sensitivity as evaluated by the homeostasis model assessment of insulin resistance (HOMA-IR).

2.2. Systolic blood pressure and total body weight

Restraint conditioning was initiated before blood pressure measurements. Systolic blood pressure (SBP) was measured in triplicate, on separate occasions throughout the day, using the tail-cuff method (Harvard Systems, Student Oscillometric Recorder, Holliston, MA, USA) [15,16] before initiation of treatment and at the end of the treatment period before killing at 21 days. Total body weights were assessed on the day of sacrifice.

2.3. Insulin sensitivity assessment

Before sacrifice, serum samples were obtained for fasting insulin and glucose measurements. The HOMA-IR was calculated as (fasting insulin [microunits per milliliter] × fasting glucose [milligrams per deciliter])/405 [22].

2.4. NADPH oxidase activity

Nicotinamide adenine dinucleotide phosphate oxidase activity was determined in plasma membrane fractions as described [16,20]. Aliquots of red gastrocnemius muscle membrane and

cytosolic fractions were incubated with NADPH (100 mmol/L) at 37°C. Nicotinamide adenine dinucleotide phosphate oxidase activity was determined by measuring the conversion of Radical Detector (Cayman Chemical, Ann Arbor, MI, USA) in the absence and presence of NADPH inhibitor diphenyleneiodonium sulfate (500 μmol/L) using spectrophotometric (450 nm) techniques.

2.5. NADPH oxidase subunit immunostaining

Harvested soleus muscle tissue was prepared as previously described [15]. Briefly, sections were incubated with 1:100 dilution goat $p47^{phox}$, Nox2 (Santa Cruz Biotechnology, Santa Cruz, CA, USA), and 1:200 of mouse anti-Rac1 antibodies in 10-fold diluted blocking agent (primary antibodies) overnight at room temperature. After washing, sections were incubated with 1:300 Alexa Fluor donkey anti-goat 647 (Invitrogen, Eugene, OR), p47, Nox2, and donkey anti-mouse for Rac1 for 4 hours. The slides, mounted with Mowiol (Millipore, Billerica, MA, USA), were examined under a biphoton confocal microscope. The images were captured with LSM imaging system, and the signal intensities were analyzed and quantified with MetaVue (Boyce Scientific, Gary Summit, MO, USA).

2.6. Oxidative stress

2.6.1. ROS tissue levels

Using isolated red gastrocnemius muscle sections, levels of ROS were measured by the lucigenin chemiluminescence technique [20]. Sections were homogenized in sucrose buffer using a glass/glass homogenizer. Homogenates were centrifuged: 1500 relative centrifugal force (rcf) × 10 minutes at 4°C. Supernatants (whole homogenate) were removed and placed on ice. Whole homogenate (100 μL) was added to 1.4 mL of 50 mmol/L phosphate (KH_2PO_4) buffer. After dark adaptation for 1 hour, samples were counted every 30 seconds for 10 minutes on a scintillation counter; and the counts for the last 5 minutes were averaged. Samples were then normalized to total protein in the whole homogenate and to day-to-day control. Values are expressed as counts per minute per milligram of protein.

2.6.2. 3-Nitrotyrosine immunostaining

3-Nitrotyrosine (3-NT) was quantified as previously described [20]. Samples were incubated with 1:20 primary rabbit polyclonal anti-nitrotyrosine antibody overnight. Sections were then washed and incubated with secondary antibodies, biotinylated linked, and labeled with streptavidin for 30 minutes each. After several rinses with Tris-buffered saline and Tween 20 (TBST), diaminobenzidine was applied for 10 minutes; and sections were rinsed several times with distilled water and stained with hematoxylin for 150 seconds, dehydrated in an ethanol series, and mounted with a permanent mounting medium. The slides were checked under a bright field microscope, the 40× images were captured with a cool snap*cf* camera, and intensities were measured with MetaVue.

2.7. Immunological analysis of IRS-1, PI3K, and IRS-1/PI3K association

Four-micrometer soleus cross-sections (n = 6 for all groups) were incubated overnight with rabbit anti-IRS-1 1:100 (Santa Cruz Biotechnology), 1:50 (phosphatidylinositol 3-kinase binding site) (BD Transduction, Lake Placid, NY) [20]. After washing several times, the sections were incubated with Alexa Flour donkey anti-rabbit 647 for IRS-1 and mounted with Mowiol. Under a biphoton confocal microscope, images were captured with LSM imaging system; and signal intensities were analyzed with MetaVue.

2.8. Dual immunological staining of IRS-1 and PI3K

After blocking of nonspecific sites, the sections were incubated with 1:50 dilution rabbit IRS-1 (Santa Cruz Biotechnology) overnight at room temperature. The following day, the sections were washed with HEPES buffer (3× 15 minutes) and incubated with 1:50 of mouse anti-PI3K (BD Transduction) in 10-fold diluted blocking agent overnight at room temperature. After washing, sections were incubated with 1:300 mixed Alexa Fluor donkey anti-rabbit and donkey anti-mouse 647 (Invitrogen) for 4 hours and mounted with Mowiol. The slides were examined under a biphoton confocal microscope, the images were captured with LSM imaging system, and the signal intensities were analyzed and quantified with MetaVue.

2.9. Co-immunoprecipitation and Western blot analysis for IRS-1 and ubiquitin

To immunoprecipitate IRS-1, red gastrocnemius tissue was powdered under liquid nitrogen and was lysed in lysis buffer; and the cell debris was removed by quick centrifugation at 3000 rpm for 5 minutes. The lysates (800 μg protein) were initially incubated with 10 μL of agarose protein G plus for 30 minutes on ice and subjected to centrifugation at 3000 rpm for 3 minutes; and the supernatant was incubated with 20 μL of agarose-conjugated mouse anti–IRS-1 antibody (Santa Cruz Biotechnology) for 5 hours at 4°C. The immunoprecipitated material was collected by centrifugation at 3000 rpm for 3 minutes, washed 3 times with phosphate-buffered saline, and resuspended in 40 μL of 2× sodium dodecyl sulfate loading buffer. Proteins were separated by sodium dodecyl sulfate polyacrylamide gel electrophoresis, transferred to nitrocellulose membrane, and probed with rabbit anti-IRS1 antibody or rabbit anti-ubiquitin antibody (Cell Signaling Technology, Danvers, MA, USA). Immunoblotting experiments were also performed using whole tissue lysates (50 μg protein).

2.10. Transmission electron microscopy

Sections of soleus muscle were thinly sliced and placed immediately in primary fixative (2% glutaraldehyde, 2% paraformaldehyde in 0.1 mol/L Na cacodylate buffer, pH 7.35). A laboratory microwave oven was used for secondary fixation with acetone dehydration and Epon-Spurr resin infiltration. Specimens were placed on a rocker overnight at room temperature, embedded the following morning, and polymerized at 60°C for 24 hours. A microtome (Ultracut UCT, Leica) with a 45° diamond knife (Diatome, Leica Microsystems, Wetzlar, Germany) was used to prepare thin (85-nm) sections. Later, the specimens were stained with 5% uranyl acetate and Sato triple-lead stain and examined with a transmission electron microscope [15,20].

2.11. Mitochondrial quantification

The same sample size (1/3 of each soleus muscle) was used in all of the experimental procedures. Animals (n = 5) were harvested, and tissues were analyzed by light microscopy. Four-micrometer paraffin-processed sections of soleus muscle strips of each treatment group (SD-C, SD-N, Ren2-C, and Ren2-N) were deparaffinized, rehydrated, and stained with complex IV subunit 1. Our soleus tissue sections were incubated with mouse anti-human complex IV subunit 1 antibody (Mitosciences, Eugene, OR) 3 μg/mL in 10-fold diluted blocker. After washing with HEPES wash buffer, the sections were incubated with 1:300 donkey anti-mouse Alexa Flour 647 (Invitrogen). After 4 hours, the sections were washed and incubated with 1:2000 DAPI. After 10 minutes, slides were washed, mounted with Mowiol, and evaluated with a multi-photon confocal system. From each section, three 63× confocal images (1040 × 1040 pixel) were captured by a biphoton confocal microscope from different areas of the sections randomly. Images were captured by LSM imaging system and enhanced with Photoshop, and mitochondria were quantified by MetaMorph (Molecular Devices, Downington, PA, USA). The images were enhanced by Photoshop (San Jose, CA, USA); and the relative number, the signal intensities, and the areas of the signals in each image were quantified by Metamorph.

2.12. Statistics

All results are presented as means ± standard error. Two-way analysis of variance with Fisher least significant differences and unpaired *t* test was performed as appropriate.

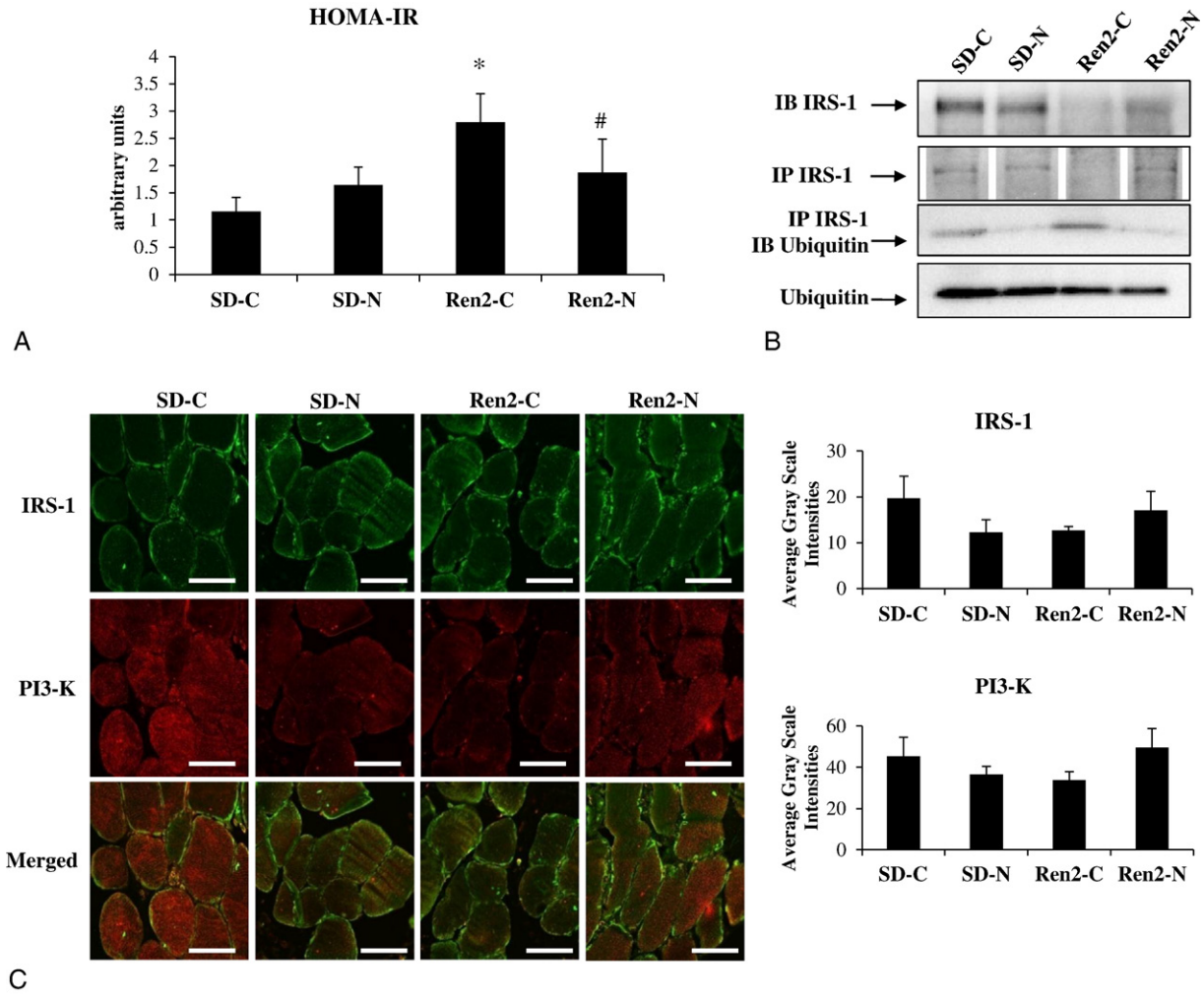

Fig. 1 – Nebivolol improves systemic insulin resistance and insulin metabolic signaling in the Ren2 rat. A, HOMA-IR was calculated as [basal insulin (milliunits per milliliter) × basal serum glucose (milligrams per deciliter)]/405 after treatment with nebivolol or placebo for 3 weeks. Sprague-Dawley control (SD-C, n = 4), SD treated with nebivolol (SD-N, n = 6), Ren2 control (Ren2-C, n = 5), and Ren2 treated with nebivolol (Ren2-N, n = 4). B, A representative image of coimmunoprecipitation and Western blot analysis for IRS-1 and IRS-1 ubiquitin association. C, Representative fluorescent images of total IRS-1, PI3K, and IRS-1/PI3K association and corresponding measures of intensity. Sprague-Dawley control (SD-C, n = 5), SD treated with nebivolol (SD-N, n = 5), Ren2 control (Ren2-C, n = 5), and Ren2 treated with nebivolol (Ren2-N, n = 5). Values are expressed as means ± SE. Scale bar, 50 μm. *P < .05 compared with SD-C. #P < .05 compared with Ren2-C.

3. Results

3.1. SBP and total body weight

As previously published [21], at initiation and end of the treatment intervention period, SBP was higher in Ren2-C group when compared with SD-C. Treatment with nebivolol resulted in a significant SBP reduction in the Ren2 compared with the nontreated animals as previously reported [21]. Nebivolol treatment for 21 days was not associated with a significant weight reduction in the Ren2 animals.

3.2. Indices of insulin sensitivity

In this investigation, we used HOMA-IR to evaluate whole-body insulin sensitivity [22]. The HOMA-IR was significantly decreased in the Ren2-C compared with SD (2.79 ± 0.5 vs 1.16 ± 0.3, $P < .05$) (Fig. 1A). Treatment with nebivolol improved whole-body insulin sensitivity in Ren2-N (1.87 ± 0.61 vs 2.79 ± 0.52, $P < .05$) compared with untreated Ren2 rats.

3.3. Total IRS-1, IRS-1, and IRS-1/PI3K association

Insulin metabolic signaling is dependent on IRS-1 engagement of the p85 regulatory component of PI3K [2,23,24]. To determine whether proteasomal degradation contributes to decreased IRS-1 and subsequent reductions in insulin metabolic signaling and downstream PI3K, we examined total IRS-1 levels by immunoblotting and by immunoprecipitation of ubiquitin. Both methods demonstrated a reduction in total IRS-1 content in the Ren2 compared with SD controls that paralleled the increased coprecipitation of IRS-1 with ubiquitin in the Ren2-C (Fig. 1B). Nebivolol treatment increased IRS-1 levels and reduced the coprecipitation of ubiquitin with IRS-1 in Ren2 animal skeletal muscle. To further characterize the protein-protein interaction between IRS-1 and PI3K, we colocalized both in soleus muscle by immunohistochemistry. However, total IRS-1 and PI3K were not

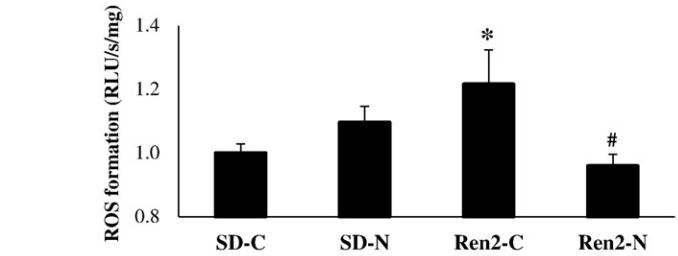

A

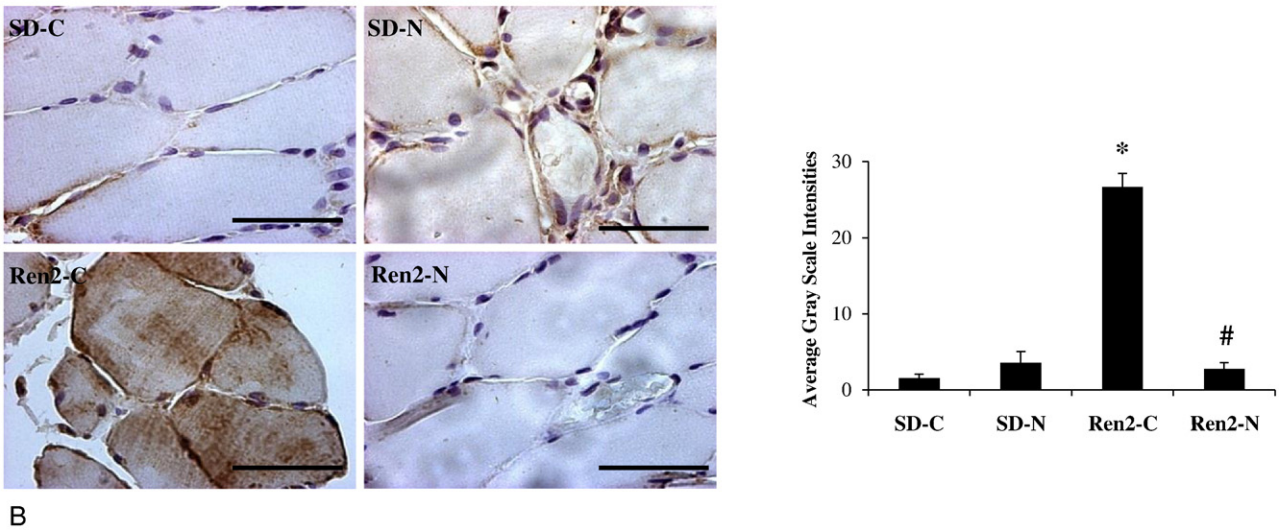

B

Fig. 2 – Nebivolol improves oxidant stress in Ren2 skeletal muscle. A, ROS formation as determined by chemiluminescence. Sprague-Dawley control (SD-C, n = 7), Sprague-Dawley treated with nebivolol (SD-N, n = 9), Ren2 control (Ren2-C, n = 7), and Ren2 treated with nebivolol (Ren2-N, n = 13). Values are presented as means ± SE. *P = .02 compared with SD-C. #P = .03 compared with Ren2-C. B, Measures of 3-NT by immunostaining and corresponding measures of intensity. Sprague-Dawley control (SD-C, n = 5), SD treated with nebivolol (SD-N, n = 5), Ren2 control (Ren2-C, n = 5), and Ren2 treated with nebivolol (Ren2-N, n = 5). Values are expressed as means ± SE. *P < .05 compared with SD-C. #P < .05 compared with Ren2-C. Scale bar = 50 μm.

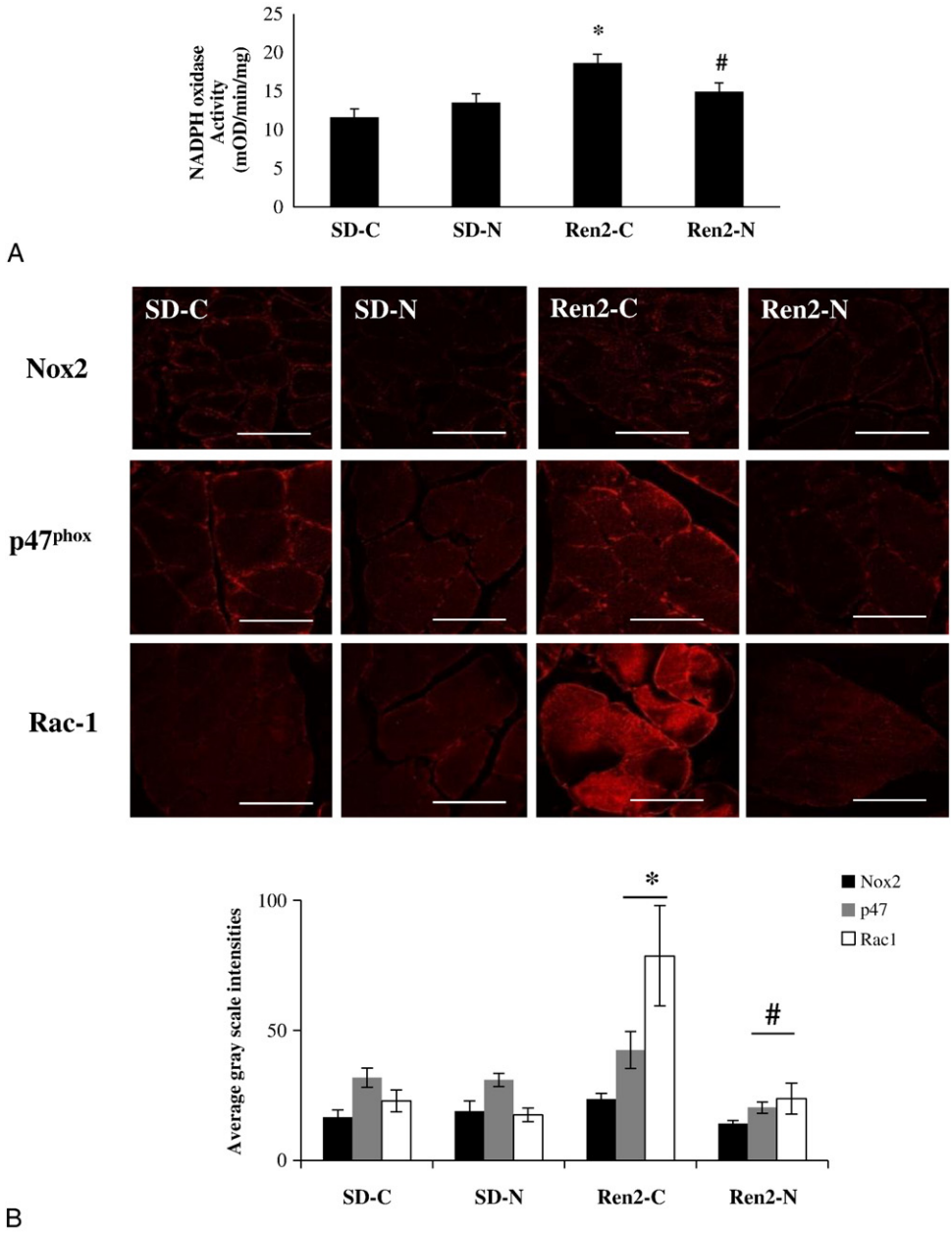

Fig. 3 – Nebivolol decreases NADPH oxidase activity and subunit expression in Ren2 skeletal muscle. A, Total NADPH oxidase enzyme activity analyzed in red gastrocnemius by spectrophotometry. B, NADPH oxidase subunits examined using immunohistochemistry. Representative images and corresponding measurements of intensity are presented. Sprague-Dawley control (SD-C, n = 5 for NADPH oxidase activity and NADPH oxidase subunits), SD treated with nebivolol (SD-N, n = 6 for NADPH oxidase activity, n = 5 for NADPH oxidase subunits), Ren2 control (Ren2-C, n = 4 for NADPH oxidase, n = 5 for NADPH oxidase subunits), and Ren2 treated with nebivolol (Ren2-N, n = 9 for NADPH oxidase, n = 5 for NADPH oxidase subunits). Values are presented as means ± SE. *P < .01 compared with SD-C. #P < .05 compared with Ren2-C. Scale bar = 50 μm.

significantly changed between groups based on signal intensities (Fig. 1C).

3.4. *Oxidative stress*

To ascertain the effects of in vivo treatment with nebivolol on ex vivo skeletal muscle oxidative stress in the Ren2, we measured total ROS levels and 3-NT content as a marker for $ONOO^-$ formation. Peroxynitrite is a highly reactive oxidant species that can be formed endogenously by the interaction of NO and superoxide anion, and this product reacts readily with tyrosine residues of proteins to form 3-NT [3,13]. The ROS levels were higher in placebo-treated Ren2 controls (1.22 ± 0.11 radio luminescence unit [RLU]/s/mg) compared with the SD group (1.0 ± 0.03 RLU/[s mg], $P = .003$). Treatment with nebivolol reduced ROS levels in Ren2-N rats

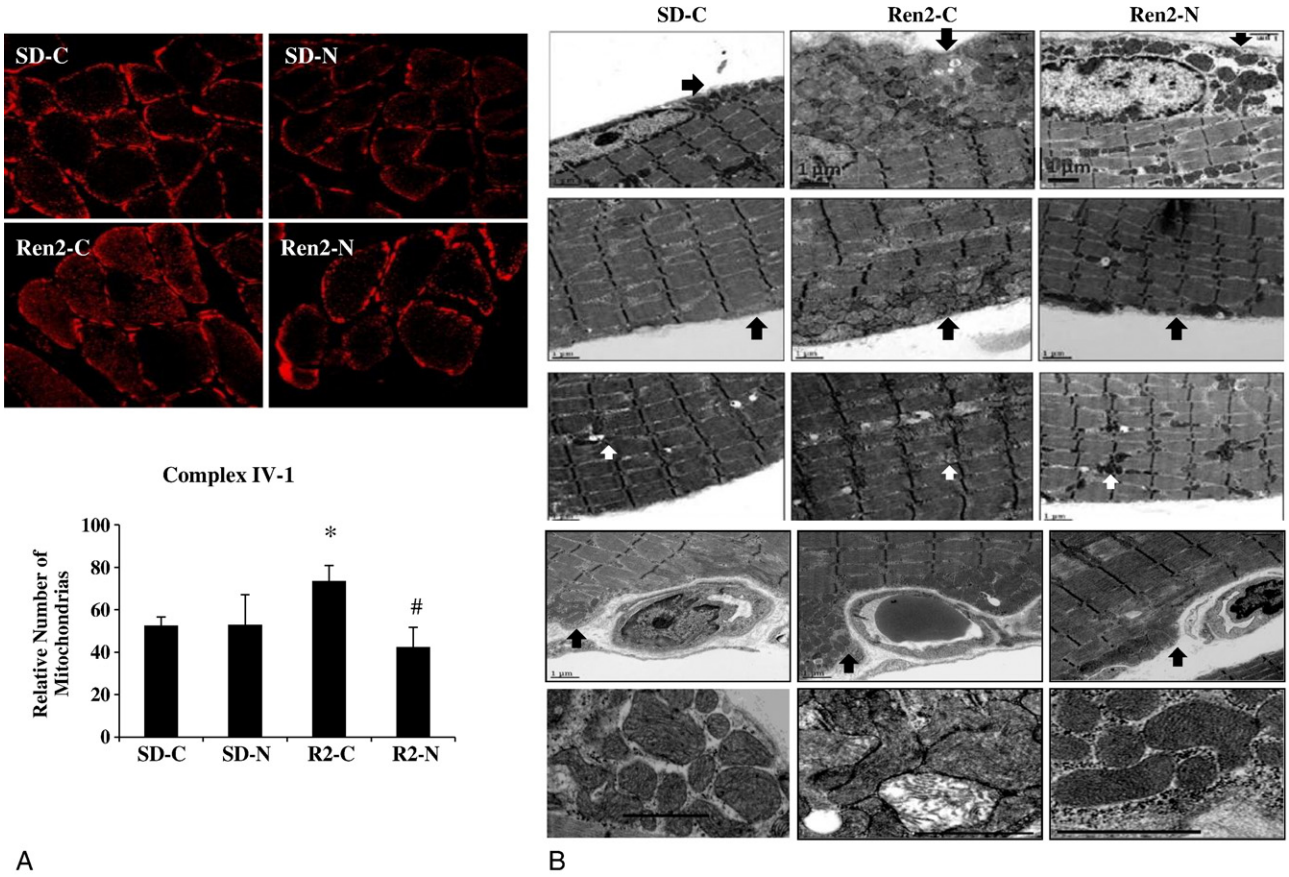

Fig. 4 – Nebivolol reduces mitochondrial density in Ren2 skeletal muscle. A, Immunohistochemistry for mitochondrial quantification (complex IV subunit 1). Values presented as means ± SE. *P < .05 compared with SD-C; #P < .05 when nebivolol-treated Ren2 (Ren2-N) rats are compared with Ren2 controls (Ren2-C). Scale bar = 50 μm. B, Representative ultrastructural examination of soleus skeletal muscle using transmission electron microscopy demonstrating increased mitochondrial number in the subsarcolemmal, intermyofibrillar, pericapillary, and perinuclear regions of the myocyte with disorganized morphology in the Ren2-C compared with SD-C. Abnormalities in Ren-2 were largely attenuated with nebivolol treatment. Arrows signal mentioned findings. Magnification, ×2500. Scale bar = 0.5 μm.

skeletal muscle (0.96 ± 0.04 RLU/[s mg], P = .02) (Fig. 2A). Furthermore, 3-NT immunostaining was increased in Ren2-C when compared with SD controls (26.8 ± 1.88 vs 1.53 ± 0.51 average gray-scale intensities, P < .05). Nebivolol reduced 3-NT immunostaining in Ren2 tissues (26.8 ± 1.88 vs 2.7 ± 0.83 average gray-scale intensities, P < .05) (Fig. 2B).

3.5. *NADPH oxidase activity*

Nicotinamide adenine dinucleotide phosphate oxidase is a primary mediator of RAAS-mediated generation of superoxide anions [9]. Nicotinamide adenine dinucleotide phosphate oxidase activity was elevated in skeletal muscle of Ren2 when compared with SD (18.6 ± 1.1 vs 1.62 ± 1.1 milli-optical density [mOD]/mg/min, P < .05) and decreased in the nebivolol-treated Ren2 rats (14.9 ± 1.1 mOD/[min mg], P < .05) (Fig. 3A). Analysis of NADPH oxidase subunits by immunohistochemistry demonstrated parallel findings, with a significantly increased Rac1 and p47 subunits in Ren2 animals compared with controls (Fig. 3B). Treatment with nebivolol for 3 weeks significantly decreased the level of p47 and Rac1 in soleus muscle samples relative to Ren2 control animals (Fig. 3B).

3.6. *Mitochondrial density*

Complex IV was measured as an indicator of total mitochondrial content [15,20,21]. This is a large transmembrane protein complex that accepts electrons from cytochrome c (eg, cytochrome c oxidase). Subunit 1 is the largest of the cytochrome c complex and is primarily responsible for heme-copper oxygenase and dioxygen-proton pumping. Immunohistostaining for complex IV subunit 1 demonstrated increases in Ren2 compared with SD controls (P < .05) and significant improvement with nebivolol treatment. As a marker for content, the complex IV subunit 1 was consistent with transmission electron microscopy analysis, which is suggestive of increased mitochondrial density with disorganized morphology in subsarcolemmal, intermyofibrillar, and perinuclear regions of the myocyte within the Ren2 (Fig. 4). These ultrastructural abnormalities in Ren-2

skeletal muscle tissue were largely attenuated with nebivolol treatment (Fig. 4).

4. Discussion

In this investigation, we examined the impact of nebivolol treatment on systemic insulin sensitivity, skeletal muscle oxidative stress, insulin metabolic signaling, and glucose uptake in a rodent model of tissue RAAS activation. Our results are commensurate with previous reports that Ren2 rats manifest impaired whole-body insulin sensitivity, enhanced skeletal muscle NADPH oxidase activity, increased ROS levels, and diminished skeletal muscle insulin signaling [6,15,16]. Data from the current investigation suggest that treatment of young insulin-resistant Ren2 rats for 3 weeks with nebivolol improves systemic insulin resistance in concert with reductions of NADPH oxidase generation of oxidative stress in skeletal muscle tissue.

Work in our laboratory with the Ren2 rat model over the last several years supports that young (6-9 weeks old) animals exhibit both systemic and skeletal muscle insulin resistance without having extensive cardiovascular and kidney disease, as do older animals. Our observation that nebivolol treatment improved insulin sensitivity in transgenic RAAS-mediated insulin-resistant rats complement prior observations in Ang II–treated [23] and overweight rodents [20], as well as insulin-resistant hypertensive persons [8,18,19,25,26]. Indeed, previous studies have demonstrated that nebivolol reduces oxidative stress and increases tissue bioavailable NO levels in cardiovascular and renal tissue [7,17,23,27]. Reduced tissue bioavailable NO levels appear to be an important factor involved in Ang II–mediated elevation of blood pressure and decreased delivery of insulin and uptake of glucose by the skeletal muscle, processes critical for skeletal muscle utilization of glucose [1,6,14-16,28]. In the context of increased tissue NADPH oxidase activity and elevated ROS levels, NO is converted to $ONOO^-$, reducing bioavailable NO levels in cardiovascular, renal, and skeletal muscle tissue [11,29].

Data generated in this investigation suggest that a treatment strategy targeting reductions in ROS in the transgenic Ren2 rat results in improved insulin metabolic signaling in soleus muscle. Reactive oxygen species generation in skeletal muscle tissue in this model is dependent on RAAS-mediated generation of the superoxide anion through NADPH oxidase activation [15,16], as well as through mitochondrial generation of ROS [21]. Effects of nebivolol treatment on NADPH oxidase activity in skeletal muscle tissue included reductions in Rac1 activation as well as decreased levels of the subunit p47. These subunits' changes accompanied reduced NADPH oxidase activity and reduced tissue levels of 3-NT. Peroxynitrite, a highly reactive oxidant species, is formed endogenously by the interaction of NO and superoxide anion; and this product reacts readily with tyrosine residues of proteins and lipoproteins to form 3-NT [9,13]. This process contributes to a reduction in bioavailable NO and also indirectly to endothelial NO synthase uncoupling, thereby further reducing bioavailable NO.

Consistent with previous reports [6,15,16], we found increased oxidative stress in skeletal muscle in the Ren2 model, a change that occurs in parallel with diminished colocalization of IRS-1and PI3K. Indeed, increased ROS levels in skeletal muscle occur contemporaneously with reductions in IRS-1 as well as increases in association of ubiquitin with IRS-1. Increased proteasomal degradation of IRS-1 in Ren2 skeletal muscle tissue occurs, in part, because of increased activation of redox-sensitive serine kinases; and this promotes serine phosphorylation and ubiquitination (and hence proteasomal degradation) of IRS-1 [3]. Our results also suggest that increases in $ONOO^-$ (measured as 3-NT) contribute to degradation of IRS-1 and impairment in insulin metabolic signaling, findings largely improved by nebivolol.

Interestingly, our data unexpectedly suggest an effect of nebivolol in healthy (SD) control rats treated with nebivolol regarding HOMA-IR and IRS-1. The underlying reasons are unclear; but these changes might reflect a differential response to the use of nebivolol in normotensive, normoglycemic, and healthy animals, as opposed to its effects on Ren2 animals, which are insulin resistant and exhibit inappropriately high oxidative stress in several tissues including skeletal muscle.

Components of the electron transfer chain are heme-containing proteins encoded by the mitochondrial genome, complex IV or cytochrome c oxidase being the most prominent [30]. In this regard, subunits I to III of cytochrome c oxidase are critical determinants of O_2 uptake and O_2^- anion formation [31]. This notion is consistent with our observation of increases in complex IV, subunit 1 (a marker of total mitochondrial content), as well as ultrastructural evidence of increased mitochondria contemporaneous with increased ROS in Ren2 skeletal muscle tissue. In this context, reductions in complex IV levels, NADPH oxidase activity, and ROS levels following nebivolol treatment may be driving the decrease in HO-1 expression in Ren2 skeletal muscle tissue.

Similar to previous studies, several ultrastructural abnormalities were observed by transmission electron microscopy in Ren2 skeletal muscle tissue, including increased number and structural abnormalities of mitochondria [15,16]. In contrast to previous reports of decreased skeletal muscle mitochondrial levels in sedentary obese and diabetic animals and humans, the current study involved a physically active and nonobese rodent model, which might explain the finding of increased mitochondria biogenesis. The increased Ren2 skeletal muscle mitochondrial biogenesis and mitochondria structural abnormalities were largely corrected by in vivo nebivolol treatment for 3 weeks. Increased mitochondrial citrate synthase and the electron transport chain activity likely also contributed to the increased levels of ROS and 3-NT in Ren2 skeletal muscle tissue. Accordingly, nebivolol may reduce oxidative stress in skeletal muscle tissue by reducing both NADPH oxidase and mitochondrial generation of ROS [21]. These reductions in oxidative stress occur in concert with improvements in insulin metabolic signaling. These results are consistent with the notion that antihypertensive treatment strategies that reduce skeletal muscle oxidative stress may help correct impaired insulin sensitivity in hypertension. In humans, earlier clinical trials validated the agent as an effective antihypertensive both when used as monotherapy and in combination with other

agents. Recent trials have reported that nebivolol is an effective antihypertensive with beneficial, or at least neutral, effects on lipids and carbohydrate metabolism [8].

In conclusion, the present investigation demonstrates that 3 weeks of treatment with nebivolol, a selective vasodilatory β_1-adrenergic receptor blocker, improves insulin resistance, reduces NADPH oxidase activity, and increases bioavailable NO in a transgenic rodent model with increased skeletal muscle oxidative stress due to enhanced activation of the RAAS. Because insulin resistance is implicated in the pathophysiology of hypertension, our findings showing improvements of insulin sensitivity with nebivolol deserve further investigation. It will be important to carry longer-term studies that examine the impact of nebivolol on insulin sensitivity and glucose metabolism in models of increased tissue RAS expression.

Funding

This research was supported by National Institutes of Health R01 HL73101-01A1 (JRS), HL-51952 (CMF), and HL59976 (WD); Veterans Affairs Merit System 0018 (JRS); Career Development Award–2 (AWC); UM Research Board (AWC); and the Forest Research Institute.

Acknowledgment

The authors wish to acknowledge the Electron Microscope Core Facility of the University of Missouri for tissue preparation.

Conflict of Interest

Disclosures: Drs Pulakat, Manrique, and Sowers have research funding from Forest Laboratories.

REFERENCES

[1] Ferrannini E, Natali A, Capaldo B, et al. Insulin resistance, hyperinsulinemia and blood pressure: role of age and obesity. European Group for the Study of Insulin Resistance (EGIR). Hypertension 1997;30:1144-9.
[2] Whaley-Connell A, Sowers JR. Hypertension and insulin resistance. Hypertension 2009;54:462-4.
[3] Cooper SA, Whaley-Connell A, Habibi J, et al. Role of renin-angiotensin-aldosterone system–induced oxidative stress in cardiovascular insulin resistance. Am J Physiol Heart Circ Physiol 2007;293:H2009-23.
[4] Manrique C, Johnson M, Sowers JR. Thiazide diuretics alone or with beta-blockers impair glucose metabolism in hypertensive patients with abdominal obesity. Hypertension 2010;55:15-7.
[5] Raitakari OT, Porkka KV, Rönnemaa T, et al. The role of insulin in clustering of serum lipids and blood pressure in children and adolescents. Diabetologia 1995;38:1042-50.
[6] Blendea MC, Jacobs D, Stump CS, et al. Abrogation of oxidative stress improves insulin sensitivity in the Ren-2 rat model of tissue angiotensin II overexpression. Am J Physiol Endocrinol Metab 2005;288:E353-9.
[7] Dessy C, Saliez J, Ghisdal P, et al. Endothelial beta 3-adrenoreceptors mediate nitric oxide–dependent vasorelaxation of coronary microvessels in response to the third-generation beta-blocker nebivolol. Circulation 2005;112: 1198-205.
[8] Fogari R, Zoppi A, Lazzari P, et al. Comparative effects of nebivolol and atenolol on blood pressure and insulin sensitivity in hypertensive subjects with type II diabetes. J Hum Hypertens 1997;11:753-7.
[9] Garrido AM, Griendling KK. NADPH oxidases and angiotensin II receptor signaling. Mol Cell Endocrinol 2009;302:148-58.
[10] Robertson RP, Harmon J, Tran PO, et al. Glucose toxicity in (2)-cells: type 2 diabetes, good radicals gone bad, and the glutathione connection. Diabetes 2003;52:581-7.
[11] Frisbee JC, Samora JB, Basile DP. Angiostatin does not contribute to skeletal muscle microvascular rarefaction with low nitric oxide bioavailability. Microcirculation 2007;14: 145-53.
[12] Frisbee JC, Samora JB, Peterson J, et al. Exercise training blunts microvascular rarefaction in the metabolic syndrome. Am J Physiol Heart Circ Physiol 2006;291:H2483-92.
[13] Pacher P, Beckman JS, Liaudet L. Nitric oxide and peroxynitrite in health and disease. Physiol Rev 2007;87: 315-424.
[14] Cole BK, Keller SR, Wu R, et al. Valsartan protects pancreatic islets and adipose tissue from the inflammatory and metabolic consequences of a high-fat diet in mice. Hypertension 2010;55:715-21.
[15] Lastra G, Habibi J, Whaley-Connell AT, et al. Direct renin inhibition improves systemic insulin resistance and skeletal muscle glucose transport in a transgenic rodent model of tissue renin overexpression. Endocrinology 2009;150:2561-8.
[16] Lastra G, Whaley-Connell A, Manrique C, et al. Low-dose spironolactone reduces reactive oxygen species generation and improves insulin-stimulated glucose transport in skeletal muscle in the TG(mRen2)27 rat. Am J Physiol Endocrinol Metab 2008;295:E110-6.
[17] Mason RP, Kubant R, Jacob RF, et al. Loss of arterial and renal nitric oxide bioavailability in hypertensive rats with diabetes: effect of beta-blockers. Am J Hypertens 2009;22:1160-6.
[18] Celik T, Iyisoy A, Kursaklioglu H, et al. Comparative effects of nebivolol and metoprolol on oxidative stress, insulin resistance, plasma adiponectin and soluble P-selectin levels in hypertensive patients. J Hypertens 2006;24:591-6.
[19] Poirier L, Cleroux J, Nadeau A, et al. Effects of nebivolol and atenolol on insulin sensitivity and haemodynamics in hypertensive patients. J Hypertens 2001;19:1429-35.
[20] Zhou X, Ma L, Habibi J, et al. Nebivolol improves diastolic dysfunction and myocardial remodeling through reductions in oxidative stress in the Zucker obese rat. Hypertension 2010;55:880-8.
[21] Whaley-Connell A, Habibi J, et al. Nebivolol reduces proteinuria and renal NADPH oxidase-generated reactive oxygen species in the transgenic Ren2 rat. Am J Nephrol 2009;30:354-60.
[22] Muniyappa R, Lee S, Chen H, et al. Current approaches for assessing insulin sensitivity and resistance in vivo: advantages, limitations, and appropriate usage. Am J Physiol Endocrinol Metab 2008;294:E15-26.
[23] Oelze M, Daiber A, Brandes RP, et al. Nebivolol inhibits superoxide formation by NADPH oxidase and endothelial dysfunction in angiotensin II–treated rats. Hypertension 2006;48:677-84.
[24] Manrique C, Lastra G, Gardner M, et al. The renin angiotensin aldosterone system in hypertension: roles of insulin

resistance and oxidative stress. Med Clin North Am 2009;93: 569-82.
[25] Pischon T, Sharma AM, Mansmann U, et al. Effect of forced titration of nebivolol on response rate in obese hypertensive patients. Am J Hypertens 2003;16:98-100.
[26] Rizos E, Bairaktari E, Kostoula A, et al. The combination of nebivolol plus pravastatin is associated with a more beneficial metabolic profile compared to that of atenolol plus pravastatin in hypertensive patients with dyslipidemia: a pilot study. J Cardiovasc Pharmacol Ther 2003;8:127-34.
[27] Mollnau H, Schulz E, Daiber A, et al. Nebivolol prevents vascular NOS III uncoupling in experimental hyperlipidemia and inhibits NADPH oxidase activity in inflammatory cells. Arterioscler Thromb Vasc Biol 2003;23:615-21.
[28] Lee-Young RS, Ayala JE, Hunley CF, et al. Endothelial nitric oxide synthase is central to skeletal muscle metabolic regulation and enzymatic signaling during exercise in vivo. Am J Physiol Regul Integr Comp Physiol 2010;298: R1399-408.
[29] Lesniewski LA, Donato AJ, Behnke BJ, et al. Decreased NO signaling leads to enhanced vasoconstrictor responsiveness in skeletal muscle arterioles of the ZDF rat prior to overt diabetes and hypertension. Am J Physiol Heart Circ Physiol 2008;294:H1840-50.
[30] Richter OM, Ludwig B. Cytochrome c oxidase—structure, function, and physiology of a redox-driven molecular machine. Rev Physiol Biochem Pharmacol 2003;147:47-74.
[31] Kim JA, Wei Y, Sowers JR. Role of mitochondrial dysfunction in insulin resistance. Circ Res 2008;102:410-4.